Am J Cancer Res 2023;13(4):1240-1258
www.ajcr.us /ISSN:2156-6976/ajcr0147874

Original Article

The expression profile of Gasdermin C-related genes predicts the prognosis and immunotherapy response of pancreatic adenocarcinoma

Xiang-Hou Xia[1,2,5*], Wen-Juan Yin[3*], Jie-Fei Mao[2], Peng Liu[4], Chen-Dong Qin[2], Jie-Jie Hu[2], Si-Yuan Liu[2], Can-Ming Wang[3], De-Hong Zou[2], Hong-Jian Yang[2], Yang Yu[2], Jian Huang[1,6,7]

[1]Department of Breast Surgery, The Second Affiliated Hospital, Zhejiang University School of Medicine, Hangzhou, Zhejiang, China; [2]Department of Breast Surgery, The Cancer Hospital of The University of Chinese Academy of Sciences (Zhejiang Cancer Hospital), Institute of Basic Medicine and Cancer (IBMC), Chinese Academy of Sciences, Hangzhou, Zhejiang, China; [3]Department of Pathology, The Cancer Hospital of The University of Chinese Academy of Sciences (Zhejiang Cancer Hospital), Institute of Basic Medicine and Cancer (IBMC), Chinese Academy of Sciences, Hangzhou, Zhejiang, China; [4]Department of Radiation Oncology, The Cancer Hospital of The University of Chinese Academy of Sciences (Zhejiang Cancer Hospital), Institute of Basic Medicine and Cancer (IBMC), Chinese Academy of Sciences, Hangzhou, Zhejiang, China; [5]Department of Breast and Thyroid Surgery, Wenling Campus of The Cancer Hospital of The University of Chinese Academy of Sciences (Zhejiang Cancer Hospital), Chinese Academy of Sciences, Taizhou, Zhejiang, China; [6]Key Laboratory of Tumor Microenvironment and Immune Therapy of Zhejiang Province, Hangzhou, Zhejiang, China; [7]Cancer Center, Zhejiang University, Hangzhou, Zhejiang, China. [*]Equal contributors and co-first authors.

Received November 19, 2022; Accepted February 16, 2023; Epub April 15, 2023; Published April 30, 2023

Abstract: Pancreatic adenocarcinoma (PAAD) has a poor prognosis and is relatively unresponsive to immunotherapy. Gasdermin C (GSDMC) induces pyroptosis in cancer cells and inflammation in the tumor microenvironment. However, whether GSDMC expression in PAAD is associated with survival or response to immunotherapy remains unknown. GSDMC expression and the relationship between GSDMC and patient survival or immune infiltration in PAAD were examined using data in the The Cancer Genome Atlas (TCGA), Gene Expression Ominbus (GEO), Genotype-Tissue Expression (GTEx) and Cancer Cell Line Encyclopedia (CCLE) databases. The TCGA PAAD cohort could be divided into two distinct risk groups based on the expression of GSDMC-related genes (GRGs). The TIDE algorithm predicted that the low-risk group was more responsive to immune checkpoint blockade therapy than the high-risk group. A novel 15-gene signature was constructed and could predict the prognosis of PAAD. In addition, the 15-gene signature model predicted the infiltration of immune cells and Immune checkpoint blockade (ICB) treatment response. Immunohistochemical staining assessment of patient-derived human tissue microarray (TMA) from 139 cases of local PAAD patients revealed a positive correlation between GSDMC expression and PD-L1 expression but a negative correlation between GSDMC expression and infiltration of low CD8+ T cells. Moreover, the overexpression of GSDMC was related to poor overall survival (OS). This study suggests that GSDMC is a valuable biomarker for predicting PAAD prognosis and predicts the immunotherapy response of PAAD.

Keywords: Gasdermin C, pyroptosis, tumor-infiltrating lymphocytes, immunotherapy, gene signature, pancreatic adenocarcinoma

Introduction

Pancreatic adenocarcinoma (PAAD) is the most common type of pancreatic cancer, accounting for more than 90% of pancreatic malignancies [1-3]. Pancreatic cancer has an age-standardized incidence rate of 5.5 per 100,000 men and 4 per 100,000 women [4]. Generally, PAAD patients have poor overall survival, with a 5-year overall survival (OS) of <10% [1-3]. PAAD is generally very resistant to routine chemotherapy and radiotherapy [5-7]. Studies have focused on how to overcome or circumvent this resistance. In 2019, the Food and Drug Administration approved the PARP inhibitor olaparib for treating pancreatic cancer with BRCA muta-

tions [8, 9]. However, BRCA1 or BRCA2 mutations are present only in 1.3-2.1% of PAADs [10]. Immunotherapy involving immune checkpoint blockade (ICB) has revolutionized the cancer treatment paradigms for many tumor types [11]. However, PAAD responds poorly to ICB [12].

Pyroptosis is an important natural immune response that plays an important role in antagonizing infection and endogenous danger signals like transformed cells [13-15]. Pyroptosis is a cell death pattern characterized by rapid cell membrane rupture and subsequent release of inflammatory mediators, such as cytokines and alarmins, inside the cell [13-15]. Therefore, pyroptosis plays a role in inflammation and immunogenicity in cancer since it induces the release of various cytokines and recruits and activates immune cells in the tumor microenvironment [16, 17]. Studies have suggested that targeting pyroptosis improves the efficacy of immunotherapy in breast cancer [18, 19]. Nevertheless, pyroptosis exhibits double-edged sword effects since inflammation (through inflammatory cytokines like IL-1 and IL-18 induced by pyroptosis) promotes tumorigenesis [20]. The role of pyroptosis and its impact on the treatment efficacy and prognosis of PAAD remains unknown.

Gasdermin C (GSDMC) is a newly identified member of the pyroptosis executioner protein family [21, 22]. GSDMC induces pyroptosis and is associated with short survival of breast cancer [23] and lung cancer [24] patients. GSDMC could be an oncogenic player in multiple cancer types [21, 25]. GSDMC appears to be an oncogene in colorectal cancer because it inhibits transforming growth factor receptor type II [26]. Studies have revealed that GSDMC is absent in normal epithelial cells [27].

Nevertheless, given the novelty of GSDMC, data about the involvement and relevance of GSDMC in PAAD remain scarce. Studies have proposed a pyroptosis-based prognostic signature in PAAD, including GSDMC expression [28, 29]. Recently, Yan et al. [30] showed that GSDMC could promote the proliferation and migration of PAAD cell lines. In addition, they developed a pyroptosis-related prognostic model based on IL18, CASP4, NLRP1, NLRP2, and GSDMC to predict the prognosis of PAAD [30]. Nevertheless, GSDMC expression in PAAD tumors and its related prognostic and therapeutic value remain unclear.

Therefore, this study aimed to investigate GSDMC expression in PAAD, the relationship between GSDMC and PAAD prognosis, and the potential of GSDMC expression to predict the immunotherapy response of PAAD. The results could help define the role of GSDMC in PAAD and its potential to predict the efficacy of immunotherapy in PAAD.

Materials and methods

Data source and processing

The TCGA dataset comprises RNA-sequencing expression profiles (level 3). The clinical information of 179 PAAD patients was obtained from the website (https://portal.gdc.com). GTEx datasets (release V8) were downloaded from the GTEx data portal website (https://www.gtexportal.org/home/datasets). The categorical data were converted to TPM and normalized to log2 (TPM+1), keeping samples with clinical information intact. An external validation cohort was obtained from the GEO database (https://www.ncbi.nlm.nih.gov/geo/, ID: GSE57495). The follow-up for the GSE57495 cohort was 4.7 years. On the other hand, the mRNA expression matrix of PAAD cell lines was downloaded from the Cancer Cell lines Encyclopedia (CCLE) dataset (https://portals.broadinstitute.org/ccle).

GSDMC expression and mutation profiles

GSDMC expression in PAAD tumor and normal tissues were analyzed using R v4.0.3 (R Foundation for Statistical Computing, Vienna, Austria). A *P*-value <0.05 was considered statistically significant. Sankey diagrams and mutation profiling of GSDMC were built using the R software packages “ggalluvial” and “maftools”, respectively. The GSDMC expression analysis of the PAAD cell lines was performed using the R v4.0.3 software package “ggplot2” (v3.3.3).

Survival analysis

The survival differences between the different GSDMC expression or risk groups of the 179 PAAD patients from the TCGA cohort and 139 PAAD patients from the TMA cohort were analyzed using the log-rank test. The accuracy of GSDMC in predicting the immunotherapy response of PAAD was evaluated using the time receiver operating characteristics (ROC) (v0.4) analysis and Kaplan-Meier curves. *P*-values and hazard ratios (HRs) with 95% confidence

intervals (CIs) were determined using log-rank tests and univariable cox proportional hazards regression analysis.

Development of a prognostic signature in the TCGA and GEO cohorts

Data were retrieved from the TCGA and GEO databases. Patients were selected from the TCGA database using the least absolute shrinkage and selection operator (LASSO) regression algorithm (10-fold cross-validation). Survival and time ROC analyses were performed as above. Analyses were performed using the R package "glmnet". Data were analyzed using multivariable Cox regression, and the iteration was performed using the step function. The most optimal model was the final model.

The expression matrix and relevant clinical features were extracted from the GSE57495 data set in the GEO database. The risk score of each sample was determined, as in the development cohort, and the samples were divided into high- and low-risk groups according to the median of 6.995.

The correlation between immune infiltration and risk score based on the gene signature

The immune scores were calculated using the QUANTISEQ algorithm. The correlations between the expression of GRGs and the immune scores were examined using the R software package "ggstatsplot" and Spearman's correlation analysis.

The difference in ICB treatment response between the different GRG risk groups and the gene signature

The TCGA PAAD cohort was classified into high/low-risk groups based on previously identified genes or the 15 genes identified in this study. The potential ICB response was predicted using the TIDE algorithm [31]. Data were analyzed using "ggplot2" (v3.3.3) and "ggpubr" (v0.4.0) packages in R (v4.0.3) software.

Tissue specimens

A total of 139 PAAD samples were obtained from the Cancer Hospital of the University of Chinese Academy of Sciences, Zhejiang Cancer Hospital (Hangzhou, China). TMA was constructed with the samples from the 139 PAAD patients as previously described [32]. Informed consent was obtained for each participant. The study was conducted according to the Helsinki declaration. The study was approved by The Ethics Committee of the Cancer Hospital of the University of Chinese Academy of Sciences (approval # IRB-2016-159(KE)).

Immunohistochemistry

Immunohistochemistry (IHC) of TMA was performed using FFPE specimens as previously described [32]. The primary antibodies used for IHC were antibodies against GSDMC (1:100, GeneTex, GTX33979), PD-L1 (1:200, GeneTex, GTX01796), and CD8 (1:100, MXB Biotechnologies, RMA-0514). Histopathological review and IHC scoring were performed by two pathologists (W.Y. and C.M.W.). GSDMC and PD-L1 were assigned positive and negative scores. CD8 was assigned with high and low scores. The expression of CD8 was considered high if >10 cells were present per high-power field (× 400).

Statistical analysis

GSDMC mRNA expression in PAAD and normal tissues were analyzed and visualized using R software v4.0.3. A *P*-value <0.05 was considered statistically significant. The OS of patients between subgroups was analyzed using the Kaplan-Meier method with a two-sided log-rank test. In addition, the prognostic value of the gene signature was evaluated using univariable and multivariable Cox regression models. Differences in immune infiltration and risk score activation between the two groups were analyzed using the Spearman non-parametric test. All statistical analyses were performed using R (v4.0.3) and relevant packages. The correlation and survival analyses in the TMA cohort were performed using IBM SPSS Statistics (Version 26).

Results

GSDMC expression and mutation profiling in PAAD

To examine the GSDMC expression in various pancreatic tissues, we compared the transcription of GSMDC mRNA in 179 tumor tissues and normal pancreatic tissues using data in the TCGA and GTEx databases. GSDMC expression was significantly higher in PAAD tumor tissues than in normal pancreatic tissues (**Figure 1A**). GSDMC expression was lower in normal (G0) tissues than in G1, G2, and G3+4 PAAD tissues

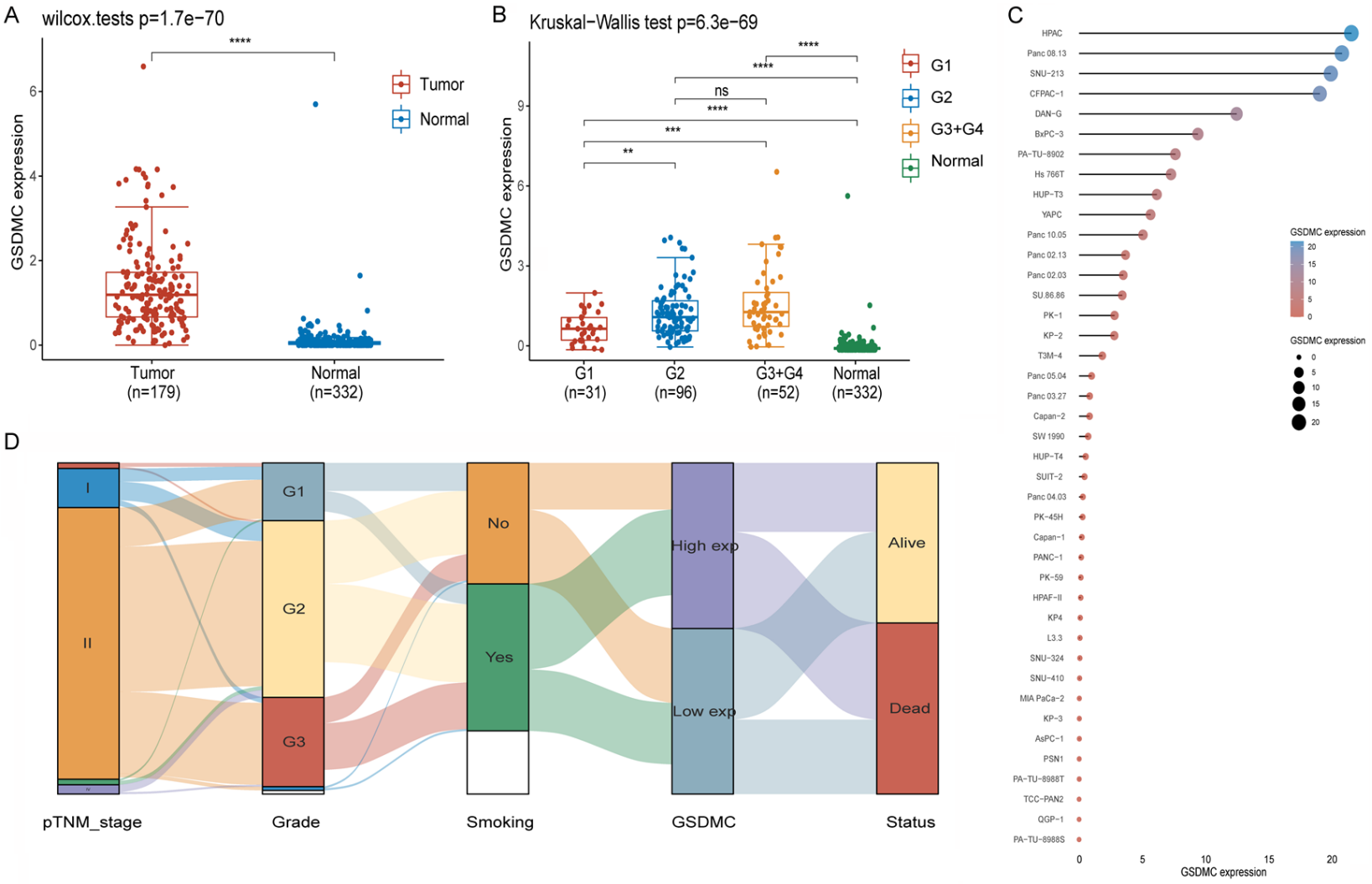

Figure 1. Differential GSDMC mRNA expression levels among various PAAD tissues or cell lines. A. Comparison of GSDMC mRNA expression levels between PAAD tumors tissues vs. normal pancreatic tissues. B. Comparison of GSDMC mRNA expression levels between normal pancreatic tissues and PAAD tumor tissues of different histological grades in PAAD. C. Comparison of GSDMC mRNA expression levels between different pancreatic cancer cell lines. D. Sangkey diagram showing GSDMC expression profile in PAAD tumor tissues categorized by different variables. Each row represents a feature variable. Different colors represent different pTNM stages. The lines represent the distribution of the same sample in different feature variables.

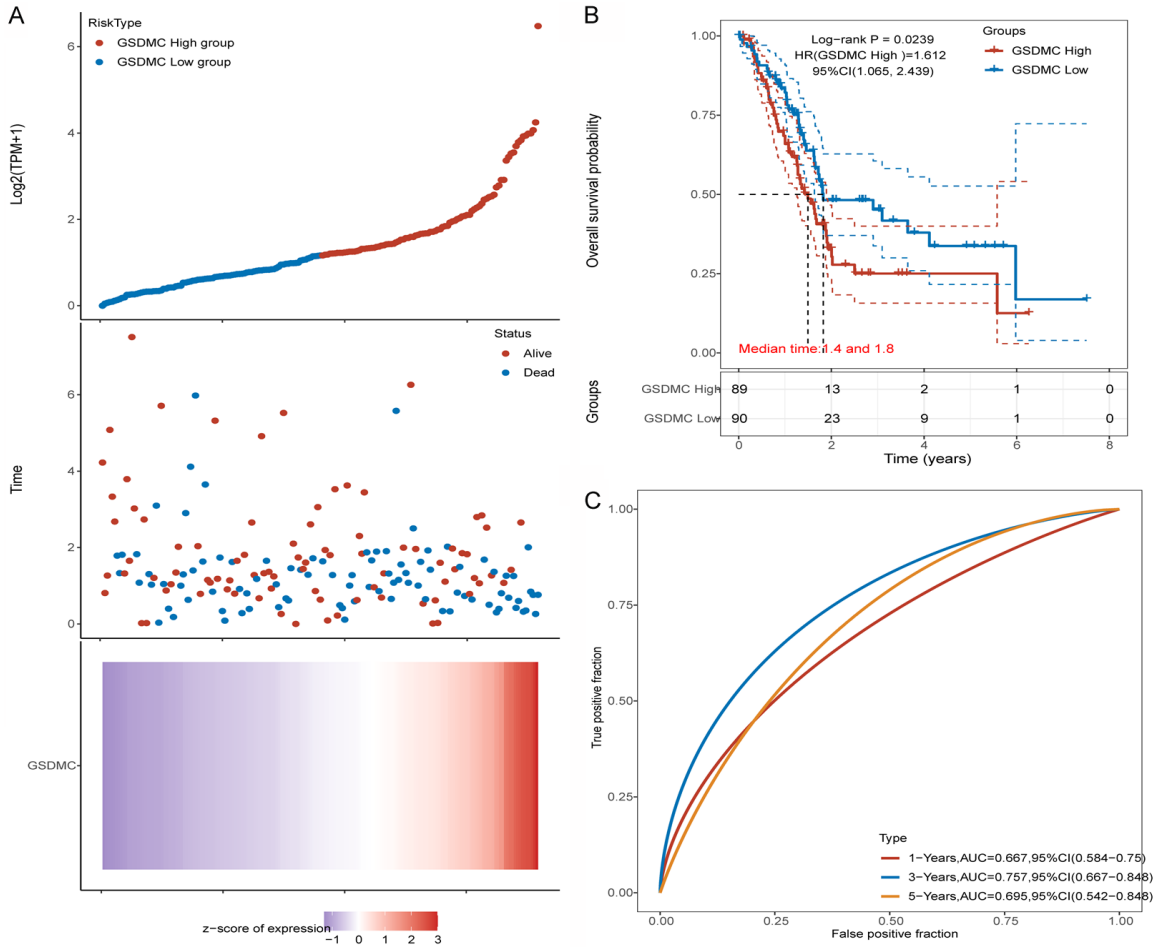

Figure 2. Correlation between GSDMC expression and overall survival of PAAD patients in the TCGA cohort. A. The gene expression, survival time, and survival status of 179 cases of PAAD from the TCGA cohort. The top scatterplot represents the gene expression from low to high. Each group is represented by a different color. The scatter plot distribution represents the gene expression of different samples with distinct survival time and survival status. The bottom figure shows the gene expression heatmap. B. Kaplan-Meier survival analysis of the gene signature from the TCGA dataset. Different groups were compared with the log-rank test. C. The receiver operating characteristics (ROC) curve of the GSDMC gene. High values indicate of high predictive power.

(**Figure 1B**), suggesting that GSDMC could participate in the initiation of PAAD development. We investigated GSDMC mRNA transcription in pancreatic cancer cell lines and found that HPAC was the most transcribed, whereas PATU-8988S was the least transcribed protein in GSDMC (**Figure 1C**). **Figure 1D** shows the Sangkey diagram of the clinical factors related to GSDMC expression. Therefore, these results suggest that high GSDMC expression is associated with PAAD.

The mutation landscape of GSDMC in the TCGA PAAD cohort generally revealed low mutation frequency in GSDMC. As shown in Supplementary Figure 1, the somatic mutation rate of GSDMC in PAAD was 0.56%. The major mutation was missense mutation, the predominant variant type was single-nucleotide polymorphism (SNP), and the single-nucleotide variation (SNV) class was C>T substitution. Therefore, the mutation rate of GSDMC in PAAD is low.

Correlation between GSDMC expression and patient OS in the TCGA cohort

The GSDMC expression was higher in PAAD tumors than in normal pancreatic tissues. Therefore, we investigated the association between GSDMC expression and OS of PAAD patients. **Figure 2A** presents the scatterplot of GSDMC expression and survival of PAAD patients. The OS was worse in the high-risk group

than in the low-risk group (median, 1.4 vs. 1.8 years, P = 0.024) (**Figure 2B**). Based on a time-dependent ROC analysis, we found that the AUC for 1-year OS was 0.667, 0.757 for 3-year OS, and 0.695 for 5-year OS (**Figure 2C**). Therefore, there is an association between GSDMC expression and the overall survival of PAAD patients.

Identification of the GSDMC-related genes (GRGs) in the TCGA cohort

To investigate the possible mechanisms underlying GSDMC effects on the overall survival of PAAD patients, we identified the GRGs in the TCGA cohort. GRGs were defined as top genes positively correlating to GSDMC and overlappingly expressed in cancers to which GSDMC was prognostically relevant. We first performed a pan-cancer analysis to investigate the impact of GSDMC on the OS across 32 cancer types in the TCGA cohorts. We found that the role of GSDMC in predicting the outcome of different types of cancer was meaningful but contradictory. High GSDMC expression was protective for low-grade glioma (LGG) but distinctly risky for PAAD (Supplementary Figure 2). Therefore, we selected LGG and PAAD as representative cancer types to identify the candidate GRGs. Using the web-tool Linkedomics (Supplementary Figure 3), we successfully identified 160 genes (Supplementary Table 1) that were positively correlated with GSDMC and were overlappingly expressed in LGG and PAAD. Out of the 160 genes, 150 (Supplementary Table 2) were identified as GRGs for further analysis.

Tumor risk classification based on the 150 GRGs and functional enrichment analysis

To validate whether the expression of GRGs predicted PAAD prognosis, we conducted a risk classification based on the 150 GRGs above. The PAAD samples in the TCGA cohort were categorized into two groups (**Figure 3A-D**). The median OS was significantly low in the high-risk group than in the low-risk group (median, 1.6 years vs. not reached, P = 0.004) (**Figure 3E**).

To unveil how GSDMC and its related genes affect the OS of PAAD patients, we examined the differences in gene functions and pathways between the high-risk and low-risk groups, which GRGs define. Based on differentially expressed gene (DEG) analysis, 10,447 DEGs were identified between the low- and high-risk groups in the TCGA cohort. Among them, 9381 genes were upregulated among high-risk individuals, while 1066 genes were downregulated (Supplementary Figure 4A, 4B and Supplementary Table 3). Gene ontology (GO) enrichment analysis and Kyoto Encyclopaedia of Genes and Genomes (KEGG) pathway analysis were performed. The results indicated that the DEGs were mainly correlated with neutrophil degranulation, neutrophil activation involved in immune response, T-cell activation, positive regulation of cytokines production and regulation of cell-cell adhesion, and cell-cell hemopoiesis (Supplementary Figure 4C, 4D). Therefore, GRGs play a role in the prognosis of PAAD.

Construction of a novel signature for PAAD OS prediction in the TCGA cohort

In light of GRGs that distinctly classified the 179 PAAD samples in the TCGA cohort into different prognostic groups, we further investigated whether GRGs could be used to construct a risk model to predict the OS of PAAD. Following the LASSO Cox regression analysis (**Figure 4A**, **4B**), a 15-gene signature was generated with the optimum λ value. The risk score was calculated as follows: risk score = (0.0486) × GSDMC + (0.1784) × RIPK2 + (0.0229) × DERA + (-0.4027) × LLGL1 + (0.1644) × BCAR3 + (0.0175) × ZFP36L1 + (0.0885) × GNA15 + (0.7983) × RGS9BP + (0.008) × S100A2 + (0.0011) × MGST1 + (0.0236) × FLNB + (-0.2548) × CC2D1B + (0.0324) × AMIGO2 + (-0.039) × GNAI2 + (0.4634) × PPP2R3A.

The median score calculated by the risk score formula divided 179 patients equally into the low- and high-risk groups (**Figure 4C**, **4E**). The OS was significantly lower in the high-risk than in the low-risk group (P<0.001) (**Figure 4D**). A time-dependent ROC analysis was performed to evaluate the sensitivity and specificity of the prognostic model, resulting in an AUC of 0.803 for 1-year OS, 0.807 for 3-year OS, and 0.918 for 5-year OS (**Figure 4F**).

Validation of 15-gene signature to predict the OS of PAAD in the GEO cohort

A total of 63 PAAD patients from a GEO cohort (GSE 57495) were used to validate the risk

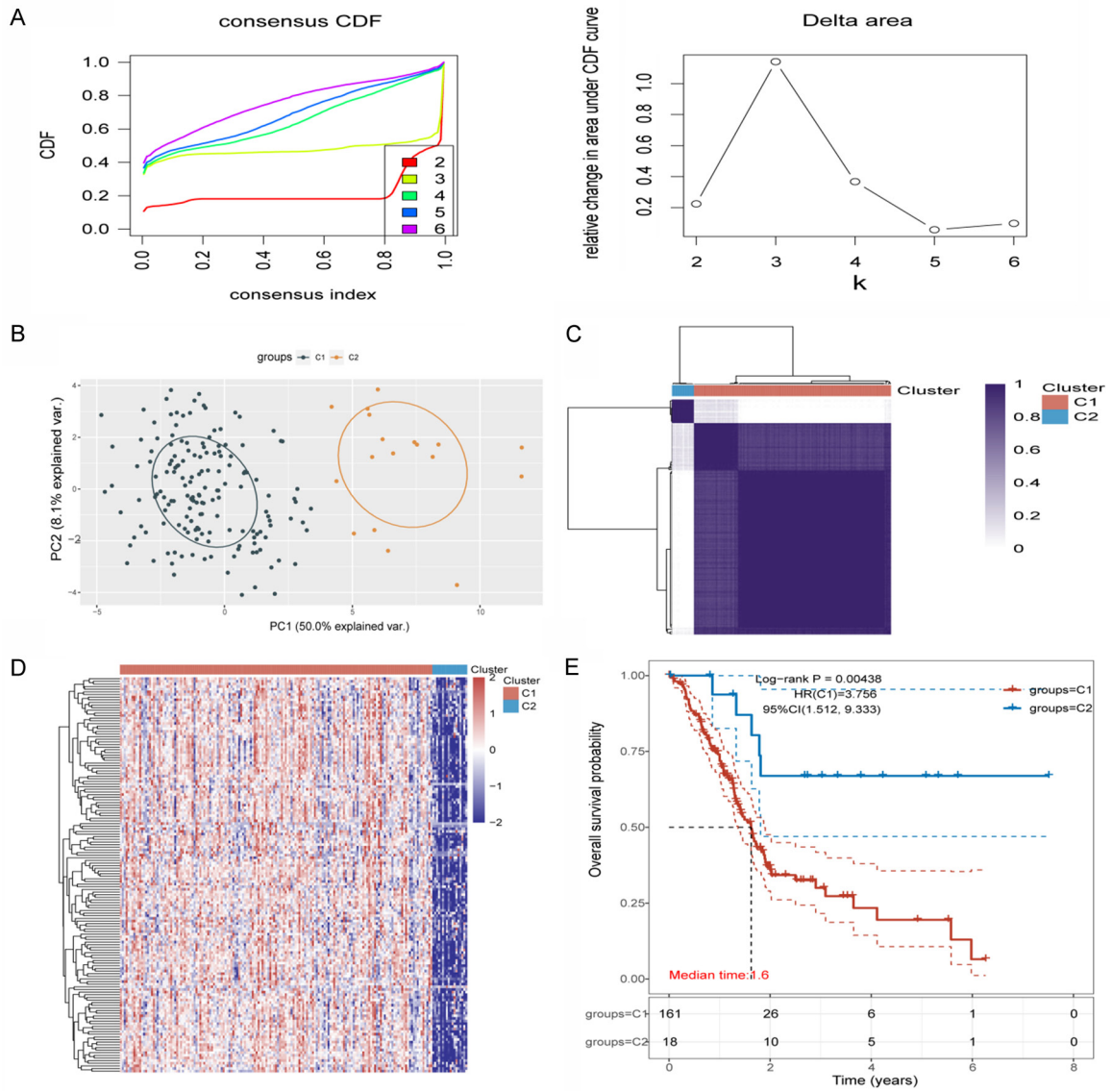

Figure 3. Tumor risk classification based on the GSDMC-related genes in the TCGA cohort. A. Consensus clustering cumulative distribution function (CDF) and relative changes in the area under the CDF curve (CDF Delta area). The relative changes in area under the CDF curves when cluster number varies between 1 and 2. The abscissa represents category number 2, and the ordinate represents the relative change in the area. B. The PCA showing satisfactory separation between the two subgroups. C. The expression heatmap of 150 genes in different subgroups. Red represents high expression, and blue represents low expression. D. Consistency among the clustering results in the heatmap (k = 150). Rows and columns represent samples. Different colors represent different types. E. Kaplan-Meier survival analysis of survival outcomes among different groups of samples in the TCGA data set. The groups was compared using the log-rank test. HR (95% CI), the median survival time (LT50) for different groups.

model built above. According to the median risk score in the TCGA cohort, 32 patients in the GEO cohort were low-risk, while 31 were high-risk (**Figure 5A**, **5B**). The Kaplan-Meier analysis revealed a poorer OS in the high-risk patients than in the low-risk patients (median, 1.5 vs. 2.5 years, P = 0.036) (**Figure 5B**). The ROC curve analysis of the GEO cohort showed good predictive accuracy (AUC = 0.633 for 1-year OS, 0.771 for 3-year OS, and 0.723 for 5-year OS) (**Figure 5C**).

Construction of a nomogram for PAAD OS prediction in the TCGA cohort

To analyze the relationship between the 15-gene signature and clinical pathological parameters in PAAD patients, we further developed a

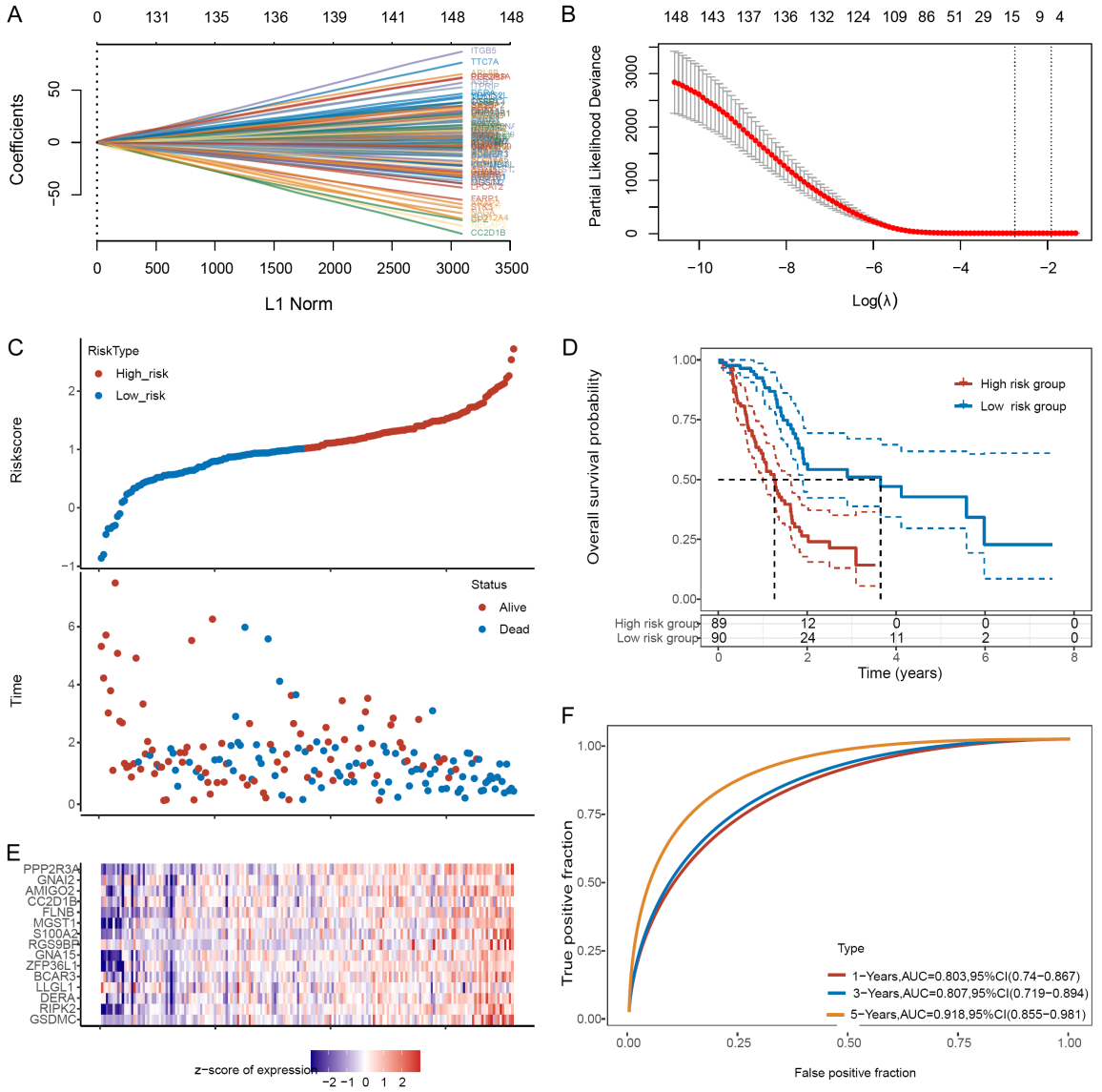

Figure 4. Construction of the risk signature based on the data of the TCGA cohort. A. The coefficient profiles of 150 GSDMC-related gene signatures are shown by lambda (λ) parameter. The abscissa represents the lambda value, and the ordinate represents the coefficients of the independent variable. B. Partial likelihood deviations were plotted against the log (λ) using the LASSO Cox regression model. C. The risk score, survival time, and survival status of PAAD cohorts for the TCGA data set. The scatterplot represents the risk score from low to high. Each group is represented by a different color. The scatter plot distribution represents the risk score of different samples corresponding to the survival time and status. Heatmap of the expression of the genes from the signature. D. Kaplan-Meier survival analysis of the risk model from the TCGA PAAD cohort, the groups were compared using the log-rank test. E. The heatmap of the gene expression from the signature. F. Time-dependent receiver operating characteristics (ROC) analysis of the 15-gene signature. High values of area under the curve (AUC) indicate highpredictive power.

nomogram based on our signature and incorporated various clinical pathological parameters (age, pT stage, pTNM stage, grade, and radiation therapy). Those clinical pathological variables and the signature were analyzed using univariate and multivariate Cox regression models, respectively (Supplementary Figure 5A, 5B). Independent prognostic variables determined by multivariate Cox regression analysis were used to construct a nomogram to predict the 1-, 3-, and 5-year OS of PAAD patients. Calibration curves were plotted and showed a great match with the actual OS of PAAD patients (Supplementary Figure 5C, 5D).

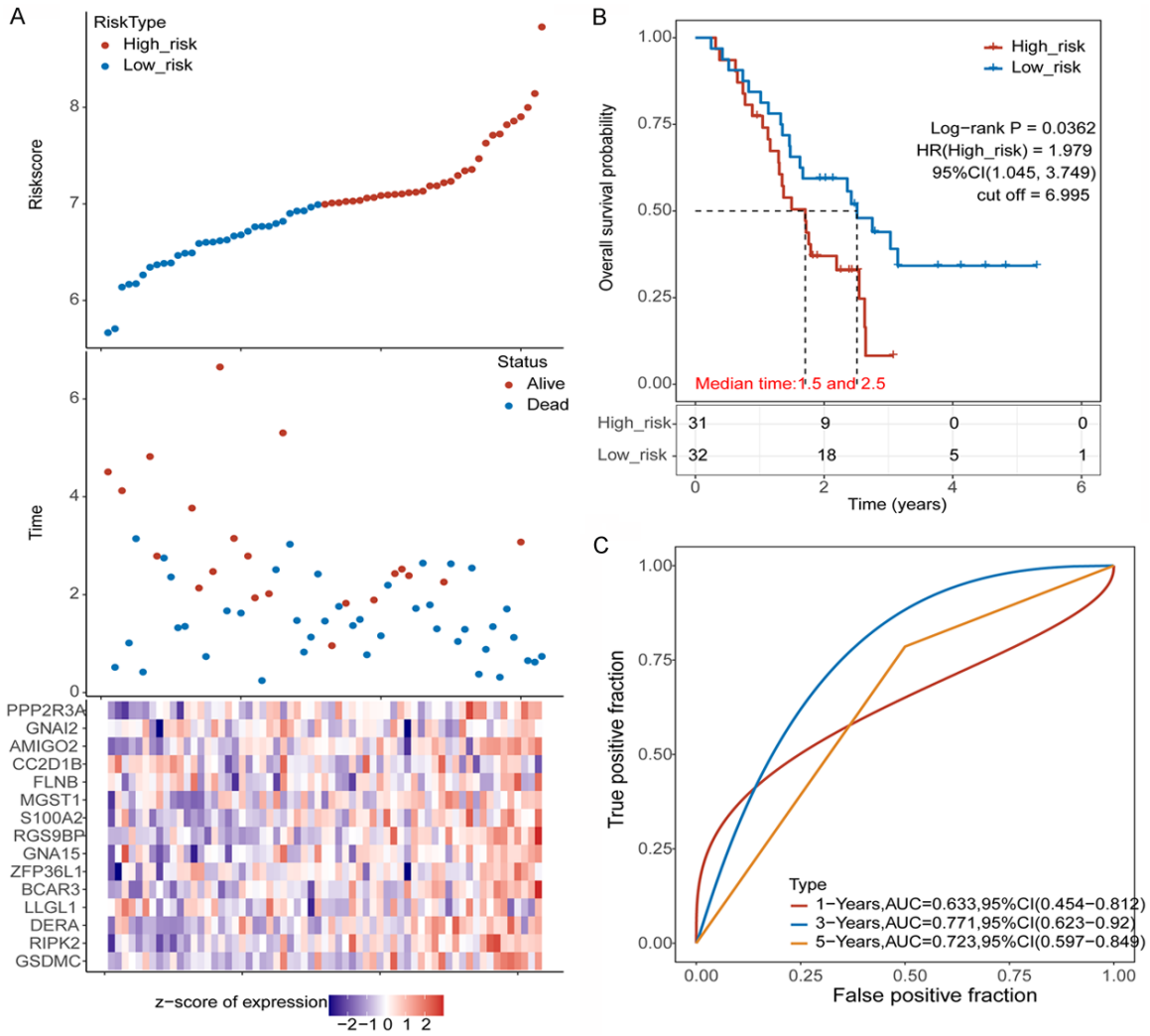

Figure 5. Validation of the 15-gene signature in the GEO cohort. A. The heatmap of risk score, survival time, survival status, and 15-gene expression profile for the validation data set. The scatterplot represents the risk score from low to high. Each group is represented by a different color. The scatter plot distribution illustrates the risk score of different samples corresponding to the survival time and status. B. Kaplan-Meier survival analysis of the survival prediction power of the risk model from the data set. Groups were compared using the log-rank test. C. Time-dependent receiver operating characteristics (ROC) analysis of the 15-gene in the validation data set.

Immune infiltration profiles based on the risk scores calculated with the 15-gene signature in the TCGA cohorts

To further investigate how the 15-gene signature classified the risk of PAAD, we analyzed the correlations between risk scores based on the 15-gene signature and the immune scores calculated using the QUANTISEQ algorithm (**Figure 6A-K**). The results showed significantly higher levels of M1 macrophages (**Figure 6B**), neutrophils (**Figure 6E**), and uncharacterized cell (**Figure 6K**) infiltration in the high-risk group than in the low-risk group. However, M2 macrophages (**Figure 6C**), monocyte cells (**Figure 6D**), NK cells (**Figure 6F**), and Myeloid dendritic cells (**Figure 6J**) were significantly lower in the high-risk group than in the low-risk group.

The response of ICB treatment between the high- and low-risk groups based on the 150 GRGs or the 15-gene signature

To investigate whether GSDMC was associated with the efficiency of ICB treatment in PAAD, we assessed the difference in potential ICB treatment responses in the high- and low-risk groups. The ICB treatment response prediction was calculated using the TIDE algorithm. A significantly more effective response to ICB was

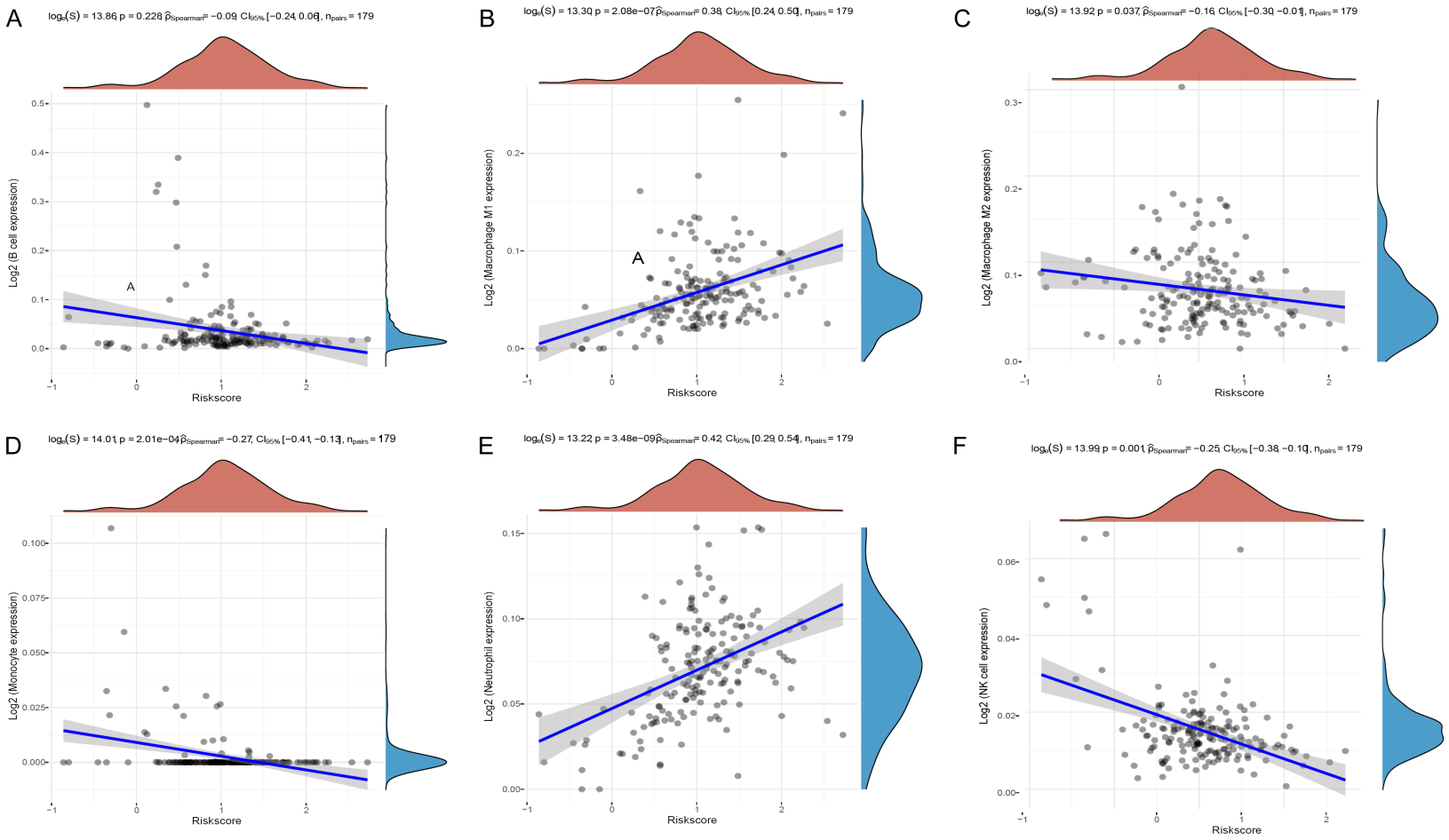
A
B
C
D
E
F
Log2 (B cell expression)
Log2 (Macrophage M1 expression)
Log2 (Macrophage M2 expression)
Log2 (Monocyte expression)
Log2 (Neutrophil expression)
Log2 (NK cell expression)
Riskscore

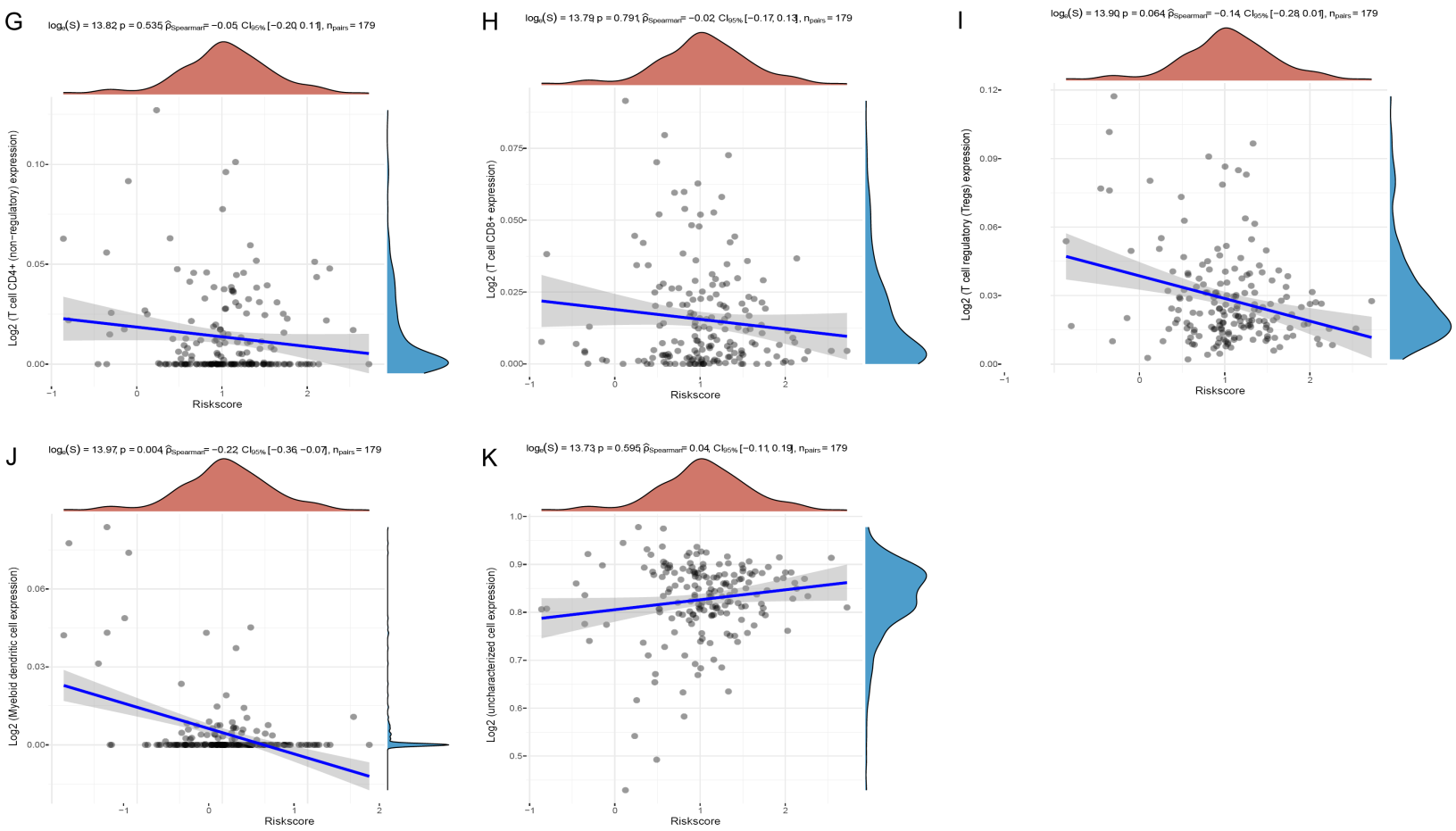

Figure 6. The correlation between immune scores and the risk score based on the 15-gene signature. Correlations were analyzed with the Spearman test. The immune scores were calculated using the QUANTISEQ immune algorithm. The abscissa represents the distribution of risk score calculated by the GRG signature, and the ordinate represents the distribution of the immune score. The density curve on the right indicates the trend in the distribution of the immune score. The upper-density curve illustrated the trend in the distribution of the gene expression or the score. The value on the top represents the correlation *p*-value, correlation coefficient, and correlation calculation.

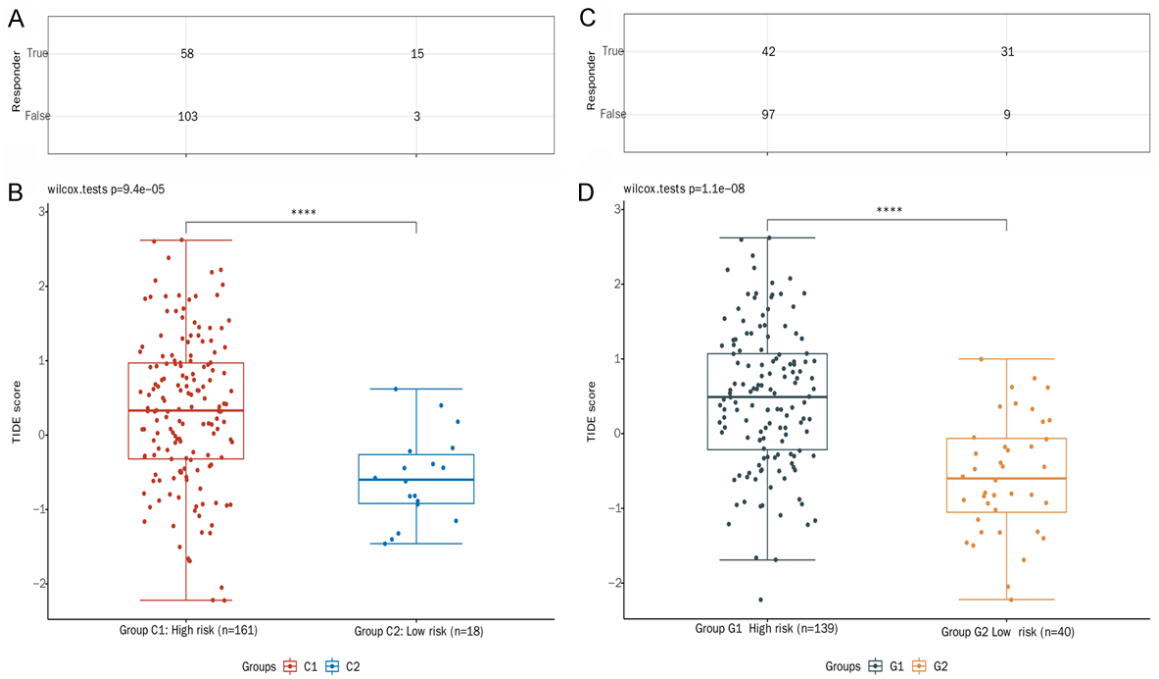

Figure 7. Response to immune checkpoint blockade treatment between classification based on 150 GRGs (left) or on 15-gene signature (right). A, C. Immune responses of samples in different groups in the prediction results. B, D. The distribution of immune response scores in different groups calculated using the TIDE algorithm. A higher TIDE score indicates lower responsive to ICB treatment.

predicted in the low-risk group than in the high-risk group based on the 150 GRGs (**Figure 7A**, **7B**) and the 15-gene signature (**Figure 7C**, **7D**).

Survival analysis based on GSDMC protein expression in the TMA cohort

We first examined GSDMC expression in 139 PAAD samples in the TMA cohort to validate the findings from the bioinformatics analyses. As shown in **Table 1**, 99 PAAD samples were GSDMC negative, while 40 were GSDMC positive. Correlations among the GSDMC expression and multiple clinicopathological factors were analyzed, and no significant difference was observed.

We then examined the correlation between GSDMC expression and the OS of 139 PAAD patients. The median OS was much longer in the GSDMC positive group than in GSDMC negative group (22 months vs. 12 months, P = 0.001) (**Figure 8**). These results were consistent with the aforementioned bioinformatic analysis, suggesting that GSDMC is a prognostic biomarker of PAAD.

Correlations between GSDMC expression and PD-L1 or CD8+ T cells infiltration in the TMA cohort

To validate the impact of GSDMC on tumor immune microenvironment in PAAD, we assessed the correlations between GSDMC expression and PD-L1 expression or CD8+ T cell infiltration in the TMA cohort. We observed that GSDMC expression was positively correlated with PD-L1 expression (R = 0.248, P = 0.003). However, GSDMC expression negatively correlated with CD8+ T cell infiltration (R = -0.177, P = 0.037) (**Figure 9** and **Table 2**). Therefore, GSDMC plays an immunosuppressive role in the tumor microenvironment of PAAD.

Discussion

The GSDMC expression in PAAD and its impact on patient prognosis and immune infiltration remain unknown. In the present study, we found that GSDMC expression was higher in PAAD than in normal pancreatic tissues. Further analysis revealed that overexpression of GSDMC expression was associated with

Table 1. Association of GSDMC expression with clinicopathological factors of patients in the PAAD TMA cohort

Factor	Total (n = 139)	GSDMC expression		
		Negative (N = 99)	Positive (N = 40)	*P* value
Gender				0.622
female	46 (33.1%)	34 (24.5%)	12 (8.6%)	
male	93 (66.9%)	65 (46.8%)	28 (20.1%)	
Age				0.503
<60	44 (31.7%)	33 (23.7%)	11 (7.9%)	
≥60	95 (68.3%)	66 (47.5%)	29 (20.9%)	
BMI				0.171
<25	117 (84.2%)	86 (61.9%)	31 (22.5%)	
≥25	22 (15.8%)	13 (9.4%)	9 (6.5%)	
Smoking				0.835
no	92 (66.2%)	65 (46.8%)	27 (19.4%)	
yes	47 (33.8%)	34 (24.5%)	13 (9.4%)	
Family history				0.836
no	54 (38.8%)	39 (28.1%)	15 (10.8%)	
yes	85 (61.2%)	60 (43.2%)	25 (18.0%)	
Tumor size				0.414
T1	16 (11.5%)	13 (9.4%)	3 (2.2%)	
T2	62 (44.6%)	41 (29.5%)	21 (15.1%)	
T3	61 (43.9%)	45 (32.4%)	16 (11.5%)	
Lymph node stage				0.810
N0	73 (52.5%)	53 (38.1%)	20 (14.4%)	
N1	49 (35.3%)	35 (25.2%)	14 (10.1%)	
N2	17 (12.2%)	11 (7.9%)	6 (4.3%)	
pTNM stage				0.639
I	27 (19.4%)	21 (15.1%)	6 (4.3%)	
II	89 (64.0%)	62 (44.6%)	27 (19.4%)	
III	21 (15.1%)	14 (10.1%)	7 (5.0%)	
IV	2 (1.4%)	2 (1.4%)	0 (0.0%)	
Histological grade				0.634
G1	22 (15.8%)	16 (11.5%)	6 (4.3%)	
G2	79 (56.8%)	54 (38.8%)	25 (18.0%)	
G3	35 (25.2%)	26 (18.7%)	9 (6.5%)	
G4	3 (2.2%)	3 (2.2%)	0 (0.0%)	

poor OS of PAAD patients. In addition, GRGs classified the TCGA PAAD cohort into two distinct risk groups. The low-risk group was more responsive to ICB therapy than the high-risk group. A novel 15-gene signature was constructed and could predict the OS based on a high- and low-risk classification. The expression of 15 genes signature was also associated with the infiltration of immune cells. Therefore, these results strongly suggest that GSDMC was upregulated in PAAD and associated with a poor prognosis of PAAD. GSDMC-related genes and the 15-gene signature could help identify patients who are more responsive to immunotherapy.

Available data suggested that GSDMC overexpression is associated with a poor prognosis in patients with breast cancer [23] and lung cancer [24]. Studies have reported that GSDMC triggers tumorigenesis in colorectal cancer [26]. Notably, GSDMC expression is low or null in normal epithelial cells [27]. Only one recent study indicated that GSDMC is also elevated in

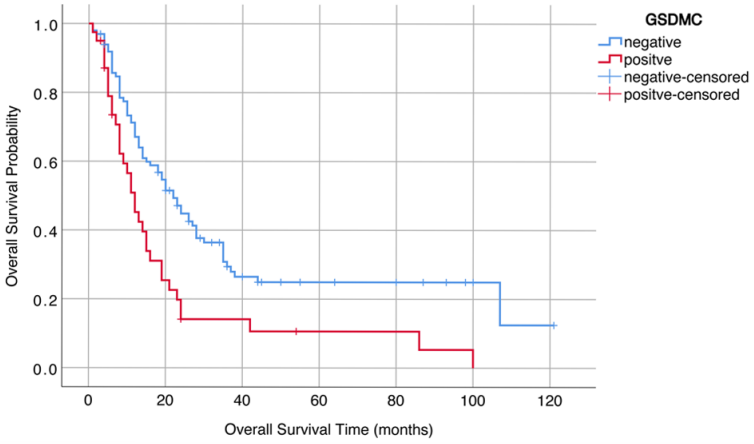

	Median OS (Months)	Std.Error	95% Confidence Interval	P-value
GSDMC negative (n=99)	22	2.562	16.978-27.022	0.001
GSDMC positive (n=40)	12	1.761	8.548-15.452	

Figure 8. Kaplan-Meier survival curve for patients with positive and negative GSDMC staining in the PAAD TMA cohort.

PAAD [30]. Therefore, since GSDMC is found mainly in cancer cells, it is a potential biomarker for different types of cancer. Nevertheless, GSDMC might have different functions in different tissues. In this study, GSDMC expression was more elevated in PAAD tissues than in normal pancreatic tissues. However, based on the data from the TGAC database, GSDMC expression was low in LGG. In addition, GSDMC overexpression was associated with a poor prognosis in PAAD patients. The present study also showed that the occurrence of mutations in the GSDMC gene in PAAD was very low (0.6%). Therefore, the GSDMC overexpression in PAAD is not due to a driving mutation in GSDMC. The driving event leading to a GSDMC overexpression remains unidentified. Pyroptosis is a type of cell death induced by inflammatory caspases (mainly caspase-1, -4, -5, and -11 [33]). These caspases activate gasdermins that migrate to the cell membrane, forming pores that lead to cell swelling and rupture, cytosol release, and pyroptosis [34]. Any endogenous and exogenous signals that activate caspase-1 can enhance pyroptosis [35]. Amplifying local and systemic inflammation will lead to pyroptosis [35]. The NLRP3 inflammasome plays a role in pyroptosis and is expressed in cancer [36]. The NLRP3 inflammasome is also activated by oxidative stress [37]. There is a need for future studies to investigate the mechanisms underlying GSDMC overexpression in PAAD.

The present study showed that the DEGs classified as GRGs were mainly enriched in immune response, T-cell activation, positive regulation of cytokines production and regulation of cell-cell adhesion, and cell-cell hemopoiesis, which are pathways associated with cancer [38, 39]. The findings of this study are consistent with the role of GSDMC in pyroptosis [23]. Pyroptosis induces inflammatory and immunogenic events in the tumor microenvironment [16, 17, 40], and the expression of genes of the GSDM family influences the PAAD microenvironment [41]. This study consistently predicted significantly higher ICB treatment responsiveness in the low-risk group than in the high-risk group classified by GRGs.

Since a molecular signature based on 150 genes is impractical in clinical application, the present study focused on the top 15 DEGs to construct a molecular signature. Besides GSDMC, the present study showed that fourteen DEGs were associated with PAAD, all of which have some relationship with cancer development. RIPK2 promotes tumor invasion and predicts cancer prognosis and immunotherapy response [42, 43]. DERA has a prognostic significance in pancreatic cancer (https://www.proteinatlas.org/ENSG00000023697-DERA/pathology/pancreatic+cancer). LLGL1 participates in cell adhesion, and the loss of LLGL1 leads to gastric cancer metastasis [44]. In addition, LLGL1 inhibits chemoresistance in PAAD [45]. BCAR3 plays a role in the prognosis of PAAD [46], ZFP36L1 promotes PAAD aggressiveness [47], GNA15 plays a role in early pancreas carcinogenesis [48], RGS9BP is among the key regulators of PAAD transcriptomics [49], and S100A2 is associated with PAAD [50]. MGST1 has recently been identified as a possible target for PAAD treatment [51]. FLNB is a potential biomarker for prostate cancer [52], and CC2D1B is an unfavorable prognostic biomarker of liver cancer (https://www.proteinatlas.org/ENSG00000154222-CC2D1B/pathology). AMIGO2 is independently

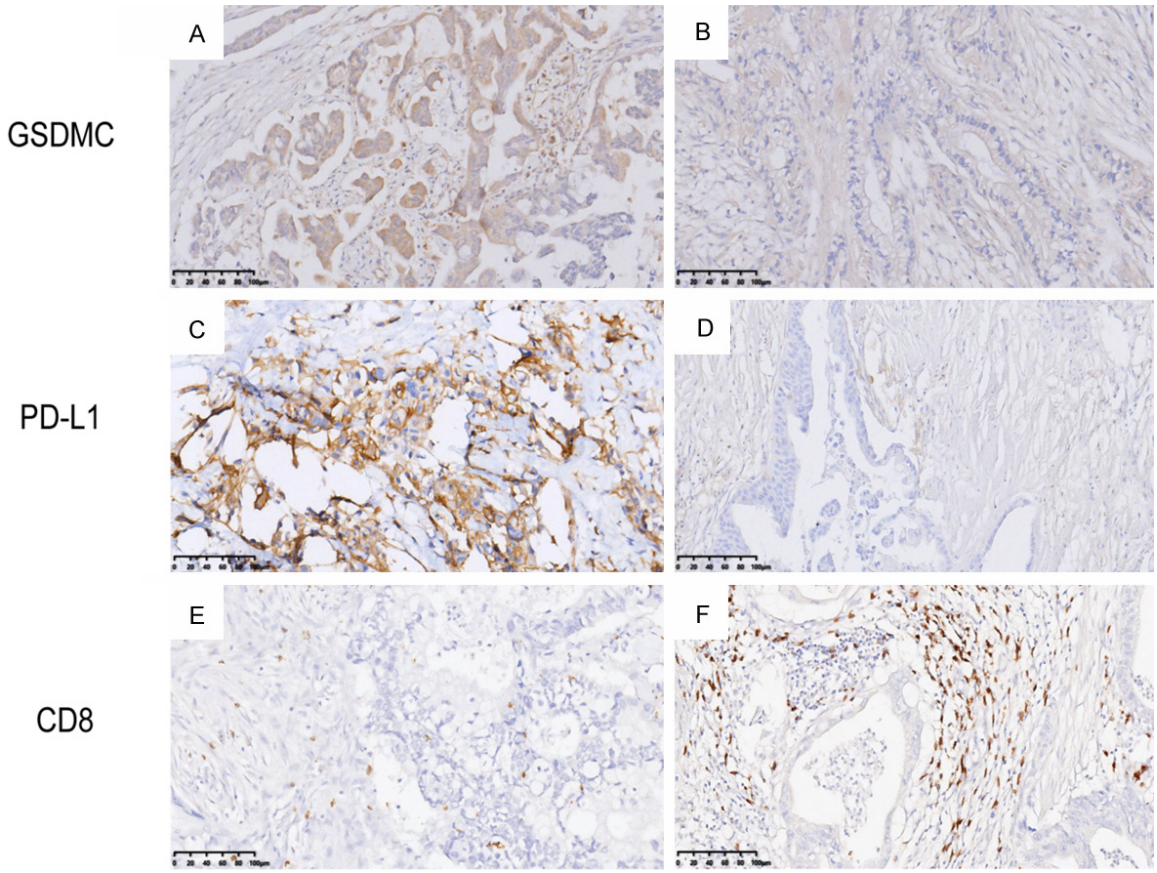

Figure 9. Representative images showing protein levels of GSDMC (positive: A; negative: B), PD-L1 (positive: C and negative: D) and infiltration of CD8+ T cells (low: E and high: F) in the PAAD TMA cohort.

Table 2. Correlation between GSDMC protein levels and PD-L1, and CD8+ T cell infiltration in PAAD patients in the PAAD TMA cohort

	GSDMC expression			*P* value	R
	Negative (N = 99)	Positive (N = 40)	total		
PD-L1				0.003	0.248
negative	91	29	120		
positive	8	11	19		
total	99	40	139		
CD8				0.037	-0.177
low	70	35	105		
high	29	5	34		
total	99	40	139		

associated with the prognosis of various solid tumors [53-55]. GNAI2 plays a role in PAAD cell migration and metastasis [56]. Finally, PPP2R3A plays a role in carcinogenesis [57]. Therefore, studies have shown that all 15 genes participate in cancer development, progression, and/or treatment response. A 15-gene signature was constructed by combining all the 15 genes, which showed discrimination for PAAD OS and biomarkers to predict the immunotherapy response of PAAD. A recent study constructed a five-gene signature based on IL18, CASP4, NLRP1, NLRP2, and GSDMC that had a good predictive value for PAAD prognosis. However, it did not examine the immunotherapy response of PAAD [30]. Song et al. [28]

constructed a prognostic signature based on 33 genes related to pyroptosis, based on CASP4 and NLRP1 but also including GSDMC, and showed that the signature was related to the OS in PAAD patients. Li et al. [29] constructed a prognostic signature based on GSDMC, CASP4, IL-18, NLRP1, NLRP2, PLCG1, and CASP1 using the TGCA database, which showed a good prognosis prediction in PAAD. Therefore, prognostic signatures that include GSDMC expression have good prediction for immunotherapy response of PAAD. There is a need to validate the signature proposed here in larger patient populations.

In addition to the OS, according to the model, the high-risk group displayed high levels of M1 macrophage and neutrophil infiltration but low M2 macrophages, NK cells, CD8+ T cells, and regulatory T cells. The low-risk group showed a better immunotherapy response to PAAD. Nevertheless, studies have shown that PAAD has a poor response to immunotherapy [58, 59]. However, some studies have suggested that combining immunotherapy with treatments that modulate the immune tumor microenvironment could lead to better responses [60, 61]. PD-L1 and GSDMC expression are linked to breast cancer and could influence the response to immunotherapy [21]. There is a need to investigate whether GSDMC or the other related genes could be modulated to enhance the immune response in immunotherapy.

This study has some limitations. Firstly, this study was primarily based on bioinformatics analyses. However, the results were validated across multiple databases using actual tissue specimens from local patients and cell lines. Secondly, our results might be compromised by confounding factors, such as different treatments, since GSDMC is reported to induce pyroptosis mainly under chemotherapy drugs. However, our analysis cohorts were not stratified by various treatments due to the very small cohort size. Finally, the mechanisms underlying GSDMC overexpression were not investigated.

In conclusion, the present study presented an in-depth analysis of the expression and effect of GSDMC on PAAD prognosis. In addition, we constructed a novel GSDMC-related signature to predict PAAD prognosis. GSDMC affects patient prognosis by reshaping the immune tumor microenvironment. This study suggests that GSDMC is a valuable biomarker for PAAD prognosis and a potential predictor for immunotherapy response in PAAD.

Acknowledgements

We thank the administrators of the TCGA database, GTEx database, GEO database, CCLE database Linkedomics and TIDE web-based database for providing data and algorithms utilized in this study. We thank Dr. Yalan Deng for revising our manuscript. This work was supported by the funds from the following projects: The National Key R&D Program of China (2022YFA1105200), National Natural Science Foundation of China (U22A0321, 81930079), Zhejiang Natural Science Research Projects (LY19H160005 andLY18H160033), and Zhejiang Provincial Science and Research Project of Traditional Chinese Medicine (2022ZB048).

Disclosure of conflict of interest

None.

Address correspondence to: Jian Huang, Department of Breast Surgery, The Second Affiliated Hospital, Zhejiang University School of Medicine, Hangzhou, Zhejiang, China. E-mail: hjys@zju.edu.cn; Yang Yu, Department of Breast Surgery, The Cancer Hospital of The University of Chinese Academy of Sciences (Zhejiang Cancer Hospital), Institute of Basic Medicine and Cancer (IBMC), Chinese Academy of Sciences, Hangzhou, Zhejiang, China. E-mail: yuyangkaiyu@163.com

References

[1] McGuigan A, Kelly P, Turkington RC, Jones C, Coleman HG and McCain RS. Pancreatic cancer: a review of clinical diagnosis, epidemiology, treatment and outcomes. World J Gastroenterol 2018; 24: 4846-4861.

[2] Kamisawa T, Wood LD, Itoi T and Takaori K. Pancreatic cancer. Lancet 2016; 388: 73-85.

[3] Kleeff J, Korc M, Apte M, La Vecchia C, Johnson CD, Biankin AV, Neale RE, Tempero M, Tuveson DA, Hruban RH and Neoptolemos JP. Pancreatic cancer. Nat Rev Dis Primers 2016; 2: 16022.

[4] Sung H, Ferlay J, Siegel RL, Laversanne M, Soerjomataram I, Jemal A and Bray F. Global cancer statistics 2020: GLOBOCAN estimates of incidence and mortality worldwide for 36 cancers in 185 countries. CA Cancer J Clin 2021; 71: 209-249.

[5] NCCN Clinical Practice Guidelines in Oncology (NCCN Guidelines). Pancreatic Adenocarcinoma. Version 1.2022. Fort Washington: National Comprehensive Cancer Network; 2022.
[6] Quinonero F, Mesas C, Doello K, Cabeza L, Perazzoli G, Jimenez-Luna C, Rama AR, Melguizo C and Prados J. The challenge of drug resistance in pancreatic ductal adenocarcinoma: a current overview. Cancer Biol Med 2019; 16: 688-699.
[7] Principe DR, Underwood PW, Korc M, Trevino JG, Munshi HG and Rana A. The current treatment paradigm for pancreatic ductal adenocarcinoma and barriers to therapeutic efficacy. Front Oncol 2021; 11: 688377.
[8] Prete AA, Procaccio L, Bergamo F, Rasola C, Nappo F, Zagonel V and Lonardi S. An unexpected tumor reduction: treatment with olaparib monotherapy in heavily pretreated BRCA2 mutated metastatic pancreatic cancer. Curr Oncol 2022; 29: 544-550.
[9] Pimenta JR, Ueda SKN and Peixoto RD. Excellent response to olaparib in a patient with metastatic pancreatic adenocarcinoma with germline BRCA1 mutation after progression on FOLFIRINOX: case report and literature review. Case Rep Oncol 2020; 13: 904-910.
[10] Lai E, Ziranu P, Spanu D, Dubois M, Pretta A, Tolu S, Camera S, Liscia N, Mariani S, Persano M, Migliari M, Donisi C, Demurtas L, Pusceddu V, Puzzoni M and Scartozzi M. BRCA-mutant pancreatic ductal adenocarcinoma. Br J Cancer 2021; 125: 1321-1332.
[11] Yang L, Ning Q and Tang SS. Recent advances and next breakthrough in immunotherapy for cancer treatment. J Immunol Res 2022; 2022: 8052212.
[12] Carpenter E, Nelson S, Bednar F, Cho C, Nathan H, Sahai V, di Magliano MP and Frankel TL. Immunotherapy for pancreatic ductal adenocarcinoma. J Surg Oncol 2021; 123: 751-759.
[13] Man SM, Karki R and Kanneganti TD. Molecular mechanisms and functions of pyroptosis, inflammatory caspases and inflammasomes in infectious diseases. Immunol Rev 2017; 277: 61-75.
[14] Strowig T, Henao-Mejia J, Elinav E and Flavell R. Inflammasomes in health and disease. Nature 2012; 481: 278-286.
[15] Fang Y, Tian S, Pan Y, Li W, Wang Q, Tang Y, Yu T, Wu X, Shi Y, Ma P and Shu Y. Pyroptosis: a new frontier in cancer. Biomed Pharmacother 2020; 121: 109595.
[16] Tan Y, Chen Q, Li X, Zeng Z, Xiong W, Li G, Li X, Yang J, Xiang B and Yi M. Pyroptosis: a new paradigm of cell death for fighting against cancer. J Exp Clin Cancer Res 2021; 40: 153.
[17] Wu J, Wang L and Xu J. The role of pyroptosis in modulating the tumor immune microenvironment. Biomark Res 2022; 10: 45.
[18] Yu H, Fu Y, Tang Z, Jiang L, Qu C, Li H, Tan Z, Shu D, Peng Y and Liu S. A novel pyroptosis-related signature predicts prognosis and response to treatment in breast carcinoma. Aging (Albany NY) 2022; 14: 989-1013.
[19] Lu L, Zhang Y, Tan X, Merkher Y, Leonov S, Zhu L, Deng Y, Zhang H, Zhu D, Tan Y, Fu Y, Liu T and Chen Y. Emerging mechanisms of pyroptosis and its therapeutic strategy in cancer. Cell Death Discov 2022; 8: 338.
[20] Balkwill F and Mantovani A. Inflammation and cancer: back to Virchow? Lancet 2001; 357: 539-545.
[21] Hou J, Zhao R, Xia W, Chang CW, You Y, Hsu JM, Nie L, Chen Y, Wang YC, Liu C, Wang WJ, Wu Y, Ke B, Hsu JL, Huang K, Ye Z, Yang Y, Xia X, Li Y, Li CW, Shao B, Tainer JA and Hung MC. PD-L1-mediated gasdermin C expression switches apoptosis to pyroptosis in cancer cells and facilitates tumour necrosis. Nat Cell Biol 2020; 22: 1264-1275.
[22] Shi J, Zhao Y, Wang K, Shi X, Wang Y, Huang H, Zhuang Y, Cai T, Wang F and Shao F. Cleavage of GSDMD by inflammatory caspases determines pyroptotic cell death. Nature 2015; 526: 660-665.
[23] Sun K, Chen RX, Li JZ and Luo ZX. LINC00511/hsa-miR-573 axis-mediated high expression of gasdermin C associates with dismal prognosis and tumor immune infiltration of breast cancer. Sci Rep 2022; 12: 14788.
[24] Wei J, Xu Z, Chen X, Wang X, Zeng S, Qian L, Yang X, Ou C, Lin W, Gong Z and Yan Y. Overexpression of GSDMC is a prognostic factor for predicting a poor outcome in lung adenocarcinoma. Mol Med Rep 2020; 21: 360-370.
[25] Wang M, Chen X and Zhang Y. Biological functions of gasdermins in cancer: from molecular mechanisms to therapeutic potential. Front Cell Dev Biol 2021; 9: 638710.
[26] Miguchi M, Hinoi T, Shimomura M, Adachi T, Saito Y, Niitsu H, Kochi M, Sada H, Sotomaru Y, Ikenoue T, Shigeyasu K, Tanakaya K, Kitadai Y, Sentani K, Oue N, Yasui W and Ohdan H. Gasdermin C is upregulated by inactivation of transforming growth factor beta receptor type II in the presence of mutated Apc, promoting colorectal cancer proliferation. PLoS One 2016; 11: e0166422.
[27] Huo CL, Deng Y and Sun ZG. A comprehensive analysis of gasdermin family gene as therapeutic targets in pan-cancer. Sci Rep 2022; 12: 13329.
[28] Song W, Liu Z, Wang K, Tan K, Zhao A, Li X, Yuan Y and Yang Z. Pyroptosis-related genes regulate proliferation and invasion of pancreatic cancer and serve as the prognostic signature for modeling patient survival. Discov Oncol 2022; 13: 39.
[29] Li L, Deng Z, Xiao Z, Zou W and Liu R. Analysis of pyroptosis-related signature for predicting

prognosis and tumor immune microenvironment in pancreatic cancer. Front Oncol 2022; 12: 770005.
[30] Yan C, Niu Y, Li F, Zhao W and Ma L. System analysis based on the pyroptosis-related genes identifies GSDMC as a novel therapy target for pancreatic adenocarcinoma. J Transl Med 2022; 20: 455.
[31] Jiang P, Gu S, Pan D, Fu J, Sahu A, Hu X, Li Z, Traugh N, Bu X, Li B, Liu J, Freeman GJ, Brown MA, Wucherpfennig KW and Liu XS. Signatures of T cell dysfunction and exclusion predict cancer immunotherapy response. Nat Med 2018; 24: 1550-1558.
[32] Deng Y, Xia X, Zhao Y, Zhao Z, Martinez C, Yin W, Yao J, Hang Q, Wu W, Zhang J, Yu Y, Xia W, Yao F, Zhao D, Sun Y, Ying H, Hung MC and Ma L. Glucocorticoid receptor regulates PD-L1 and MHC-I in pancreatic cancer cells to promote immune evasion and immunotherapy resistance. Nat Commun 2021; 12: 7041.
[33] Bergsbaken T, Fink SL and Cookson BT. Pyroptosis: host cell death and inflammation. Nat Rev Microbiol 2009; 7: 99-109.
[34] Martinon F and Tschopp J. Inflammatory caspases and inflammasomes: master switches of inflammation. Cell Death Differ 2007; 14: 10-22.
[35] Martinon F, Mayor A and Tschopp J. The inflammasomes: guardians of the body. Annu Rev Immunol 2009; 27: 229-265.
[36] Zhang H, Li L and Liu L. FcgammaRI (CD64) contributes to the severity of immune inflammation through regulating NF-kappaB/NLRP3 inflammasome pathway. Life Sci 2018; 207: 296-303.
[37] Hoseini Z, Sepahvand F, Rashidi B, Sahebkar A, Masoudifar A and Mirzaei H. NLRP3 inflammasome: its regulation and involvement in atherosclerosis. J Cell Physiol 2018; 233: 2116-2132.
[38] Wang Q, Li P and Wu W. A systematic analysis of immune genes and overall survival in cancer patients. BMC Cancer 2019; 19: 1225.
[39] Wang Y, Wang H, Yao H, Li C, Fang JY and Xu J. Regulation of PD-L1: emerging routes for targeting tumor immune evasion. Front Pharmacol 2018; 9: 536.
[40] Yu P, Zhang X, Liu N, Tang L, Peng C and Chen X. Pyroptosis: mechanisms and diseases. Signal Transduct Target Ther 2021; 6: 128.
[41] Tang R, Liu X, Liang C, Hua J, Xu J, Wang W, Meng Q, Liu J, Zhang B, Yu X and Shi S. Deciphering the prognostic implications of the components and signatures in the immune microenvironment of pancreatic ductal adenocarcinoma. Front Immunol 2021; 12: 648917.
[42] Song J, Yang R, Wei R, Du Y, He P and Liu X. Pan-cancer analysis reveals RIPK2 predicts prognosis and promotes immune therapy resistance via triggering cytotoxic T lymphocytes dysfunction. Mol Med 2022; 28: 47.
[43] Yang Q, Tian S, Liu Z and Dong W. Knockdown of RIPK2 inhibits proliferation and migration, and induces apoptosis via the NF-kappaB signaling pathway in gastric cancer. Front Genet 2021; 12: 627464.
[44] Desuki A, Staib F, Gockel I, Moehler M, Lang H, Biesterfeld S, Maderer A, Galle PR, Berger MR and Schimanski CC. Loss of LLGL1 expression correlates with diffuse gastric cancer and distant peritoneal metastases. Can J Gastroenterol Hepatol 2019; 2019: 2920493.
[45] Zhu YX, Li CH, Li G, Feng H, Xia T, Wong CH, Fung FKC, Tong JH, To KF, Chen R and Chen Y. LLGL1 regulates gemcitabine resistance by modulating the ERK-SP1-OSMR pathway in pancreatic ductal adenocarcinoma. Cell Mol Gastroenterol Hepatol 2020; 10: 811-828.
[46] Zhang ZM, Wang JS, Zulfiqar H, Lv H, Dao FY and Lin H. Early diagnosis of pancreatic ductal adenocarcinoma by combining relative expression orderings with machine-learning method. Front Cell Dev Biol 2020; 8: 582864.
[47] Yonemori K, Seki N, Kurahara H, Osako Y, Idichi T, Arai T, Koshizuka K, Kita Y, Maemura K and Natsugoe S. ZFP36L2 promotes cancer cell aggressiveness and is regulated by antitumor microRNA-375 in pancreatic ductal adenocarcinoma. Cancer Sci 2017; 108: 124-135.
[48] Innamorati G, Wilkie TM, Malpeli G, Paiella S, Grasso S, Rusev B, Leone BE, Valenti MT, Carbonare LD, Cheri S, Giacomazzi A, Zanotto M, Guardini V, Deiana M, Zipeto D, Serena M, Parenti M, Guzzi F, Lawlor RT, Malerba G, Mori A, Malleo G, Giacomello L, Salvia R and Bassi C. Galpha15 in early onset of pancreatic ductal adenocarcinoma. Sci Rep 2021; 11: 14922.
[49] Hossain SMM, Halsana AA, Khatun L, Ray S and Mukhopadhyay A. Discovering key transcriptomic regulators in pancreatic ductal adenocarcinoma using Dirichlet process Gaussian mixture model. Sci Rep 2021; 11: 7853.
[50] Ohuchida K, Mizumoto K, Miyasaka Y, Yu J, Cui L, Yamaguchi H, Toma H, Takahata S, Sato N, Nagai E, Yamaguchi K, Tsuneyoshi M and Tanaka M. Over-expression of S100A2 in pancreatic cancer correlates with progression and poor prognosis. J Pathol 2007; 213: 275-282.
[51] Dodson M, Anandhan A and Zhang DD. MGST1, a new soldier of NRF2 in the battle against ferroptotic death. Cell Chem Biol 2021; 28: 741-742.
[52] Narain NR, Diers AR, Lee A, Lao S, Chan JY, Schofield S, Andreazi J, Ouro-Djobo R, Jimenez JJ, Friss T, Tanna N, Dalvi A, Wang S, Bunch D, Sun Y, Wu W, Thapa K, Gesta S, Rodrigues LO, Akmaev VR, Vishnudas VK and Sarangarajan

R. Identification of Filamin-A and -B as potential biomarkers for prostate cancer. Future Sci OA 2016; 3: FSO161.

[53] Goto K, Morimoto M, Osaki M, Tanio A, Izutsu R, Fujiwara Y and Okada F. The impact of AMIGO2 on prognosis and hepatic metastasis in gastric cancer patients. BMC Cancer 2022; 22: 280.

[54] Han Z, Feng Y, Deng Y, Tang Z, Cai S, Zhuo Y, Liang Y, Ye J, Cai Z, Yang S, Liang Y, Hon CT, Chen J and Zhong W. Integrated analysis reveals prognostic value and progression-related role of AMIGO2 in prostate cancer. Transl Androl Urol 2022; 11: 914-928.

[55] Izutsu R, Osaki M, Jehung JP, Seong HK and Okada F. Liver metastasis formation is defined by AMIGO2 expression via adhesion to hepatic endothelial cells in human gastric and colorectal cancer cells. Pathol Res Pract 2022; 237: 154015.

[56] Wang Y, Li H and Li F. ELMO2 association with Galphai2 regulates pancreatic cancer cell chemotaxis and metastasis. PeerJ 2020; 8: e8910.

[57] Cunningham CE, Li S, Vizeacoumar FS, Bhanumathy KK, Lee JS, Parameswaran S, Furber L, Abuhussein O, Paul JM, McDonald M, Templeton SD, Shukla H, El Zawily AM, Boyd F, Alli N, Mousseau DD, Geyer R, Bonham K, Anderson DH, Yan J, Yu-Lee LY, Weaver BA, Uppalapati M, Ruppin E, Sablina A, Freywald A and Vizeacoumar FJ. Therapeutic relevance of the protein phosphatase 2A in cancer. Oncotarget 2016; 7: 61544-61561.

[58] Cheng X, Zhao G and Zhao Y. Combination immunotherapy approaches for pancreatic cancer treatment. Can J Gastroenterol Hepatol 2018; 2018: 6240467.

[59] Yoon JH, Jung YJ and Moon SH. Immunotherapy for pancreatic cancer. World J Clin Cases 2021; 9: 2969-2982.

[60] Mellman I, Coukos G and Dranoff G. Cancer immunotherapy comes of age. Nature 2011; 480: 480-489.

[61] Winter H, van den Engel NK, Ruttinger D, Schmidt J, Schiller M, Poehlein CH, Lohe F, Fox BA, Jauch KW, Hatz RA and Hu HM. Therapeutic T cells induce tumor-directed chemotaxis of innate immune cells through tumor-specific secretion of chemokines and stimulation of B16BL6 melanoma to secrete chemokines. J Transl Med 2007; 5: 56.

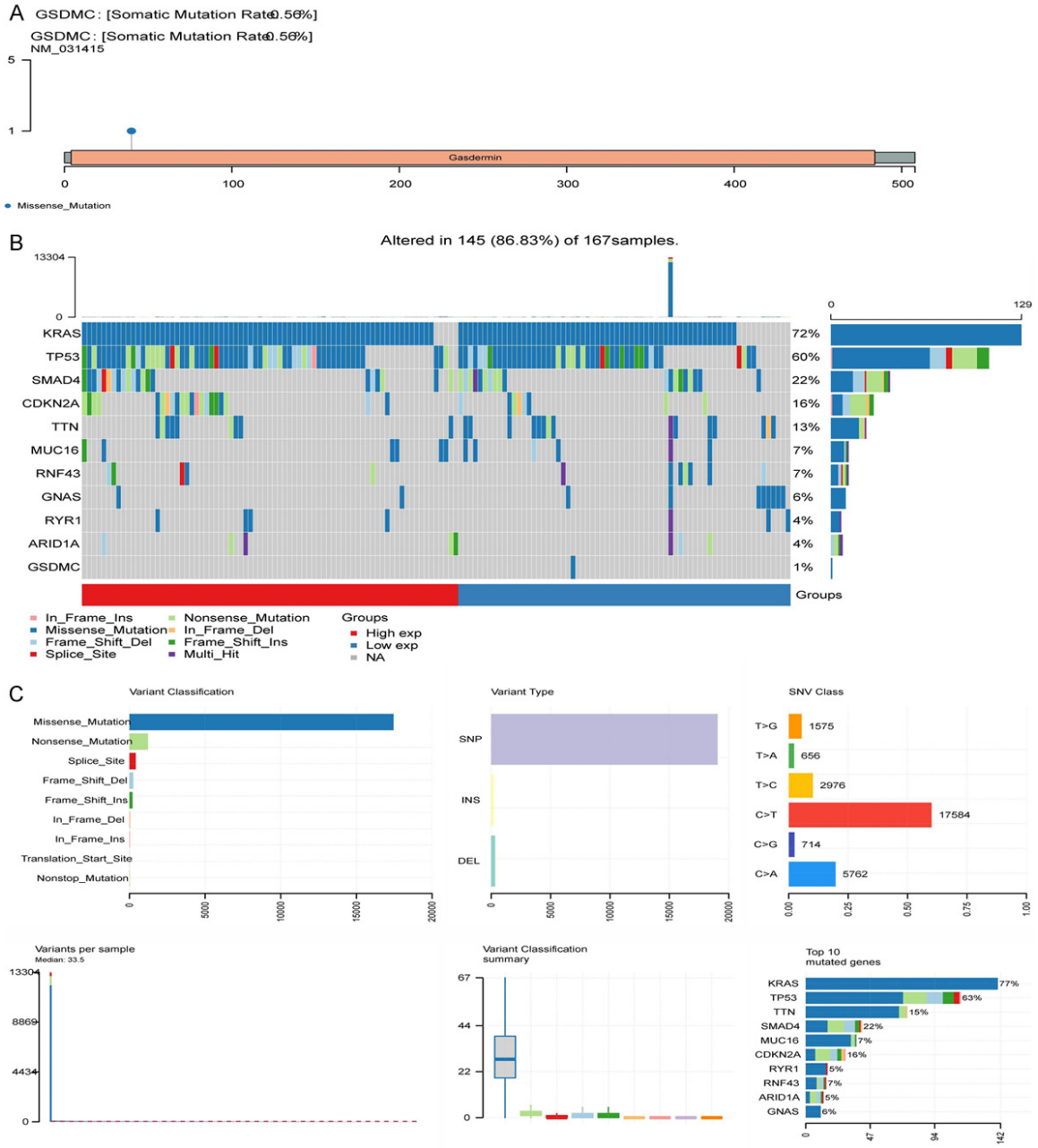

Supplementary Figure 1. GSDMC mutation landscape in the PAAD TCGA cohort. A. Mutation diagram of GSDMC in PAAD across protein domains. B. GSDMC Somatic landscape in the TCGA PAAD tumor cohort. The genes are ordered by their mutation frequencies. The samples are ordered by disease histology, as indicated by the annotation bar (bottom). The sidebar plot shows the -log10-transformed q-values, as estimated using Mut SigCV. The waterfall plot shows mutation information for each gene for each sample. The bar plot above the legend shows the mutation burden. C. Cohort summary of the distribution of variants according to variant classification, type, and SNV class. The bottom part (from left to right) indicates the mutation load of each sample (variant classification type). The stacked bar graph shows the top ten mutated genes.

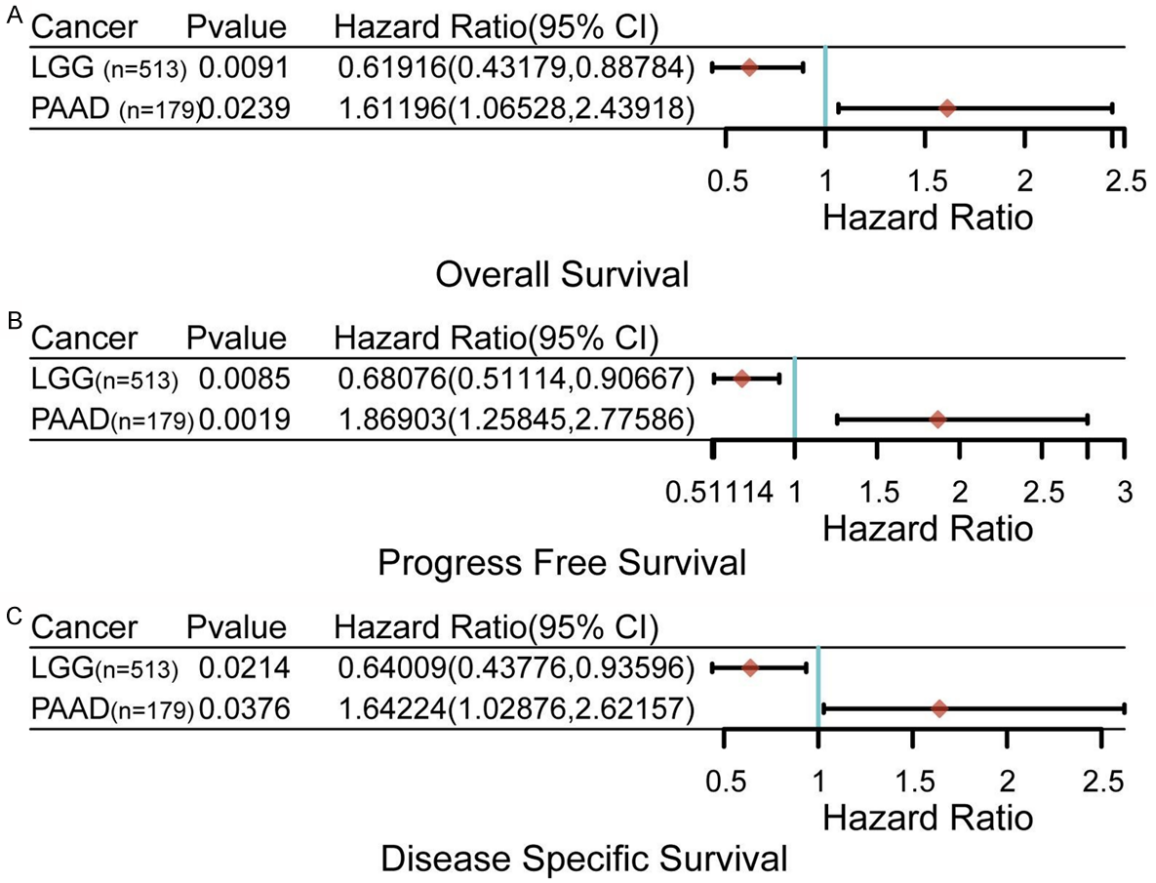

Supplementary Figure 2. Associations between GSDMC expression and patients survival in LGG and PAAD. Forest plots showing associations between GSDMC expression and overall survival (A), progress free survive (B) and disease specific survival (C) in LGG and PAAD. Univariate cox regression analysis and the forest was used to show the *P* value, HR and 95% CI of each variable through 'forestplot' R package. All the analysis methods and R package were implemente by R version 4.0.3. Two-group data were performed by wilcox test. *P* values less than 0.05 were considered statistically significant (*P<0.05).

Supplementary Figure 3. Screenshots of the parameters selected to obtain the candidate GSDMC-related genes on the Linkedomics website.

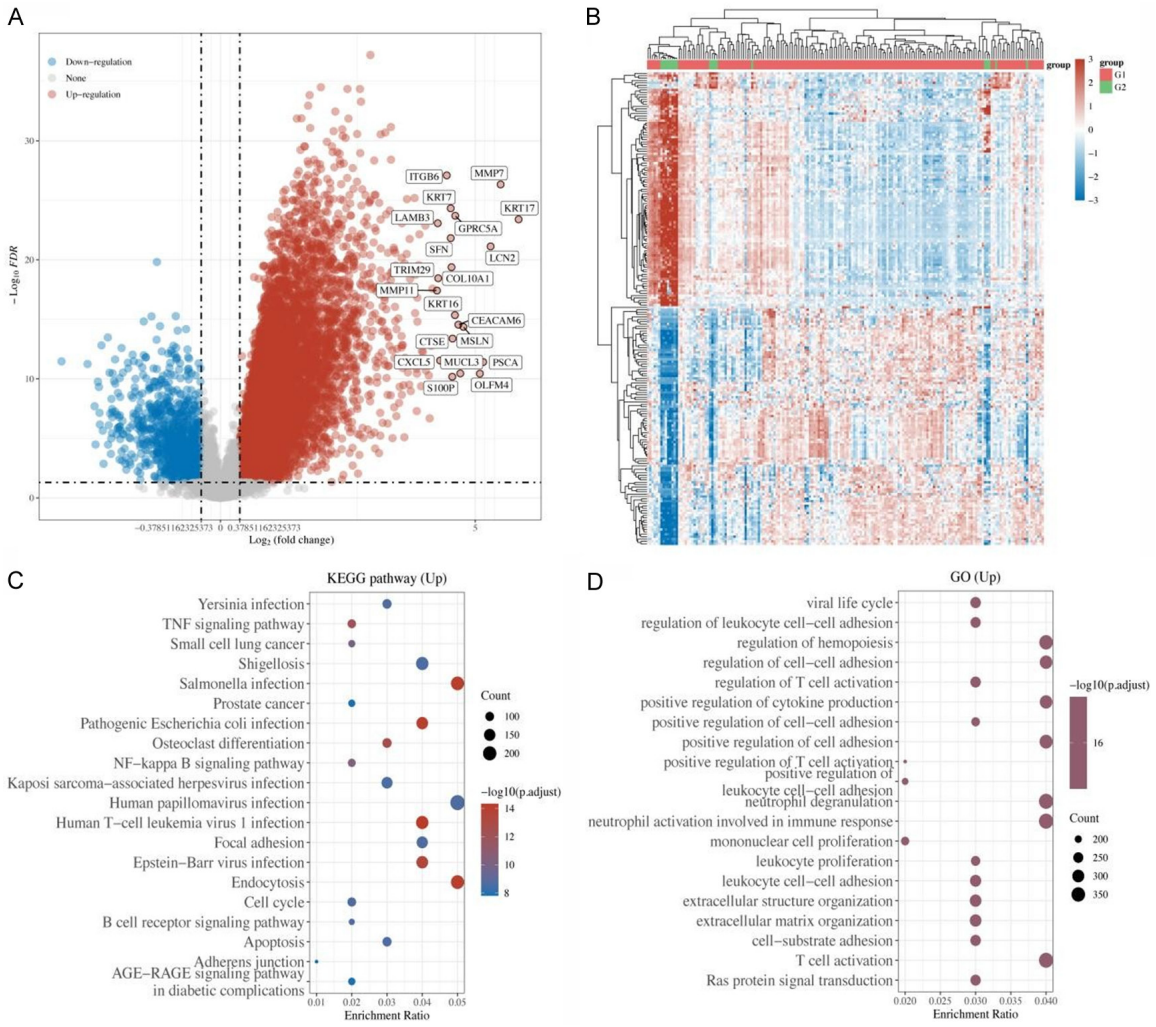

Supplementary Figure 4. Functional enrichment of differentially expressed genes between the high- and low-risk groups based on the GRGs. A. The volcano plot was constructed using a 1.3-fold change and *P*-value <0.05. The red dots indicate upregulated genes. The blue dots indicate down-regulated genes. The grey dots indicate no significant genes. B. The heatmap of the differential gene expression. Each group is reprented by a different color. The top 50 up-regulated genes and top 50 down-regulated genes are shown in this figure. C and D. The enriched KEGG signaling pathways were selected to demonstrate the primary biological actions of potential major mRNA. The abscissa indicates gene ratio, and the enriched pathways are presented in the ordinate. Gene ontology (GO) analysis of potential targets of mRNAs. The biological process (BP), cellular component (CC), and molecular function (MF) of potential targets were clustered based on the "Cluster Profiler" package in R software (version: 3.18.0). The colors represent the significance of differential enrichment. The size of the circles represents the number of genes; the larger the circle, the greater the number of genes. In the enrichment result, FDR<0.05 is considered to be a meaningful pathway (enrichment score with -log10 (P) of more than 1.3).

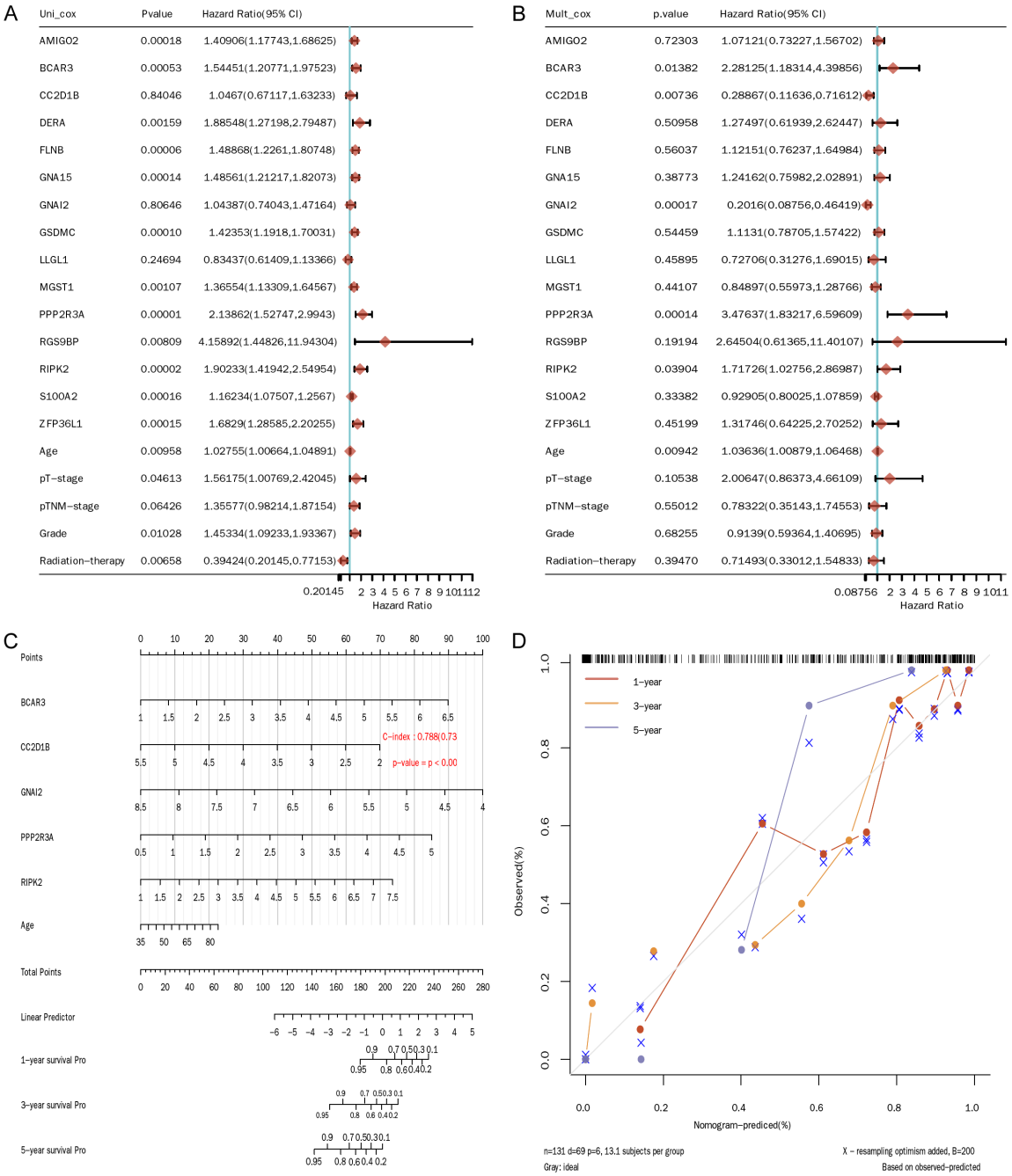

Supplementary Figure 5. Nomogram based on the 15-gene signature. Univariate (A) and multivariate (B) Cox regression. Nomogram can predict the 1-year, 3-year and 5-year overall survival of PAAD patients. (C) Calibration curve for the overall survival nomogram model. (D) The dashed diagonal line represents the ideal nomogram, and the blue line, red line and orange line represent the 1-year, 3-year and 5-year of the observed nomogram.